A theoretical tool that predicts the nature of the 4f states of Ce compounds

H. C. Herper[1], T. Ahmed[3], J. M. Wills[2], I. Di Marco[1],
I. Locht[1], D. Iusan[1], A. V. Balatsky[3] and O. Eriksson[1]

[1] *Department of Physics and Astronomy,*
Uppsala University, Box 516,
751 20 Uppsala, Sweden

[2] *Theoretical Division,*
Los Alamos National Laboratory,
Los Alamos, NM 87545, USA

[3] *Center for Integrated Nanotechnologies,*
Los Alamos National Laboratory,
Los Alamos, NM 87545, USA

Abstract

We present a systematic study of the hybridization function of a large body of Ce compounds aiming to classify the systems depending on their itinerant character. For more than 350 data sets of cubic Ce compounds (included in the IMS data base) the hybridization function has been analized from density functional theory using a full-potential approach. We demonstrate that the strength of the hybridation function evaluated in this way allows to make precice conclusion about the level of itineracy or localiztion of the 4f states. The theoretical results are entirely consistent with all experimentral information regarding degree of 4f localization, for all investigated materials. A strong anti-correlation between the size of the hybridization function and the volume of the systems has been observed. The *information entropy* for this set of systems amounts to ~ 0.42. This means a high predictive power which could be used to tailor new materials with desired properties. This holds also for the Kondo physics in these systems. The calculated hybridization temperatures together with the density of states reproduce the expected exponential behavior if compared to Kondo temperatures obtained from experiments and allows for predictions which systems may qualify themselves as Kondo systems.

PACS numbers: 71.15Mb, 71,20Dg, 72.15Rn, 74.70Xa

I. INTRODUCTION

Cerium is the most abundant rare earth and it has found its way in many fields of applications. CeO_2 for example is used for catalysis in combustion engines[1] or as an abrasive in glass or lenses manufacturing[2]. More recently Ce has been used in laser technology, i.e. in crystal lasers (Li-Sr-Al-F-Ce) which are used to detect air pollution[3]. Ce is also used for steel hardening processes or in Al coatings.[4–6] Depending on the application, Ce-based compounds with different materials properties are needed, and since the electronic structure often is decisive in determining these properties, the understanding of the degree of localization-delocalization of the 4f shell is crucial. In fact, it is important to understand the degree of localization-delocalization of the f-shell, in general, for lanthanide- and actinide-compounds. Several materials improvements are expected from this knowledge, e.g. rare-earth-lean permanent magnets where the contribution from 4f states to the magnetic anisotropy energy in general is big, and determined by the nature of the 4f states. Ce compounds have been investigated in great detail experimentally as well as theoretically and numerous applications have been found[7] However, to identify new materials for a special purpose or with certain materials properties is a bit like searching for a needle in a haystack. Aiming to tailor Ce based materials with desired property, in particular to decide the degree of localization-delocalization, we have performed extensive high-throughput calculations in which we have linked the electronic properties of the materials to a tuneable materials specific parameter; the hybridization function. As demonstrated here, this allows to identify among all known cubic Ce compounds the correct level of itineracy of the 4f shell, a finding that is likely to carry over also to other f-electron systems.

It should be noted that the ambition to identify criteria with which to distinguish if the 4f shell is itinerant or not, have been discussed in the past. In this discussion, the so called Hill plot is the most famous one. Hill identified a correlation between magnetism and superconductivity for f-based systems (Ce and U) and the atomic distance. A beautiful relationship was found such that smaller atomic distances were found in compounds that had superconductivity, whereas materials with large distances displayed magnetism[8]. To be precise, Hill observed that superconductivity did not occur for compounds with Ce-Ce distance larger than 3.4 Å and that magnetism did not occur for materials with Ce-Ce distance smaller than 3.4 Å. For U compounds the critical distance, the Hill-limit, was 3.5

Å. Although the correlation observed by Hill was excellent, some exceptions have been found, e.g. in $CeRh_3B_2$ and URh_3, that both have large distance between Ce (or U) atoms, while the expected magnetism is absent in both compounds. This has motivated other measures that involve interatomic distances in Ce based compounds, in order to predict properties, see e.g. Ref. [9,10].

In its most straight forward form, the question concerning delocalized or localized f-electron behavior is determined by the competition between energy gain due to band formation, and energy cost due to the fact that when itinerant electrons move through the lattice they sometimes occupy the same lattice site, with an increased Coulomb repulsion, the Hubbard U. This competition in interactions may be quantified via the Hubbard model, which in the approximation of dynamical mean field theory[11,12] is considered in terms of the Anderson impurity problem. In this problem, the Hubbard U enters naturally, and the band formation may be translated into a hybridization function, or simply put, the hybridization of a localized 4f level with orbitals centered on surrounding atoms. We will in this work focus on the hybridization function, since as we shall se, it naturally gives information about the degree of localization. In addition, the hybridization function allows for estimates of the Kondo temperature, via the expression $J_{\mathrm{K}} \propto \Delta^2/(E_F - E_f)$, where J_{K} is the interaction between f- and valence states, E_F is the Fermi level, E_f the energy of the 4f level, and Δ the hybridization.[13,14] Properties normally observed for Ce compounds, like RKKY exchange interaction, Kondo singlet formation, and valence fluctuations are normally associated to J_{cf}; for smaller values the 4f electrons are essentially localized and can develop interatomic exchange via the RKKY coupling. For increasing values of J_{K} the Kondo effect becomes dominant, so that a singlet many-body state develops. Even larger values of the hybridization function pushes Ce systems into a itinerant regime, with fully delocalized bands.[15,16]

The decisive parameters for J_{cf} are the position of the 4f level with respect to the Fermi level, and the hybridization between 4f states and the remaining valence electrons. Both these properties are actually available from ab-initio electronic structure theory. The first by calculations of the valance stability, using the Born-Haber cycle,[17,18] whereas the second may be evaluated from the so called hybridization function. As a result of the different values of J_{K}, a plethora of characteristic behaviors have been identified for Ce compounds where the starting point of the electroinc structure is that of a localized 4f shell that interacts more or less strongly with surrounding electron stares. As examples we mention that materials with

dominant RKKY interaction are antiferromagnets, although exceptions to this exists, e.g. CePdSb[19] and $CeRu_2Ge_2$[20] that both show a ferromagnetic ordering. CePtIn and CeNiIn seem to have stronger interaction, hybridization, and have been characterized as so called *dense* Kondo system, without any observed magnetic ordering down to low temperatures[21]. In addition, $Ce_3Bi_4Pt_3$ is also a Kondo system, although for this material a hybridization gap has been observed.[22] On top of these effects, the interesting effect of heavy fermion superconductivity has been observed,[23] e.g. in $CeCu_2Si_2$, $CeCoIn_5$ and $CeRu_2Si_2$. Among the most strongly hybridized materials where itinerant 4f electrons have been proposed one finds, e.g. α-Ce, $CeRh_3$, CeN and $CeFe_2$.[15,16,24,25]

In the present work we make an attempt to correlate known experimental characteristics of the electronic structure of a large set of Ce compounds (366 to be exact) with information obtained from electronic structure theory, i.e. the hybridization function, in order to distinguish between localized and delocalized 4f electron behavior. For a few of the investigated materials where we identify the 4f shell to be only weakly hybridized, we have also calculated J_{cf} and compared the calculated values to experimental data of the Kondo temperature. One of the current trends in electronic structure theory is the efficiency and reliability of theory[26] combined with the ability to generate large data bases of electronic structures and related information, e.g. as demonstrated in Ref. 27. The present work shows that this approach is useful when combined with concepts from many-body model Hamiltonians, and that predictions can be made even for complex phenomena of correlated electron physics.

II. METHODS

The electronic structure of 366 binary cubic Ce compounds has been investigated within density functional theory (DFT) calculations using a full potential linear muffin tin orbitals (LMTO) as implemented in the RSPt code.[28] andthe data are now part of the IMS database for 4f and 5f systems ? If not stated otherwise the structural input data have been extracted from the Inorganic Crystal Structure Database (ICSD)[29] by using cif2cell[30]. Alloys and systems containing deuterium or tritium which were also present in the ICSD as well as systems with large unit cells (50 > atoms) have not been included in our investigations. All calculations have been performed within the generalized gradient approximation (GGA)

in the formulation of Armiento and Mattsson (AM05)[31,32] neglecting spin-polarization and spin-orbit coupling effects. This approximation is not expected to influence drastically the main object of focus of this investigation, the hybridization function. A discussion of the errors made by these assumptions can be found in the Appendix. All calculations have been performed on a similar level of accuracy (the GGA level), which is important when trying to identify trends over large sets of compounds.

The k-point meshes of the different cells have been generated according to the length of the reciprocal lattice vector in 1/Å divided by 0.15 to ensure a comparable k-point density for all systems. The energy has been converged to 10^{-14} Ry. For comparison a number of binary and ternary reference systems with different geometries has been taken into account using the same convergence parameters and k-point densities. The hybridization function $\Delta(E)$ which is used to classify the Ce compounds is obtained from single shot RSPt calculations using an energy point mesh of 1501 points and a Fermi smearing of 1mRy.

III. RESULTS

A. The hybridization function

In a quantum impurity model (Andersson) the energy-dependent hybridization function $\Delta(E)$ is part of the bath surrounding the impurity cluster. The hybridization function describes the interaction of an impurity electron – in our case the 4f electron of Ce – with the bath consisting of all other electrons. Let G_0 be the site projected Green's function calculated from density functional theory, H the impurity Hamiltonian that does not contain hybridization, with corresponding energy E^{QI}. Then we obtain via the Dyson equation an expression for the hybridization function, $\Delta(E)$, via

$$\mathrm{G}_0^{-1} = (E - E^{\mathrm{QI}}) - \Delta(E) = (E - H) - \Delta(E). \quad (1)$$

In the quantum impurity Andersson model, the hybridization function can be viewed as a measure of the tendency for band formation of the Ce 4f electron. The larger the hybridization function the bigger the overlap of the 4f orbital with orbitals of the other electrons, which in principle should be guiding parameter for how itinerant the system is.

The results of the hybridization function of a large set of Ce compounds is presented below, in a way that groups compounds naturally. In Fig. 1(a) we show data for the well-

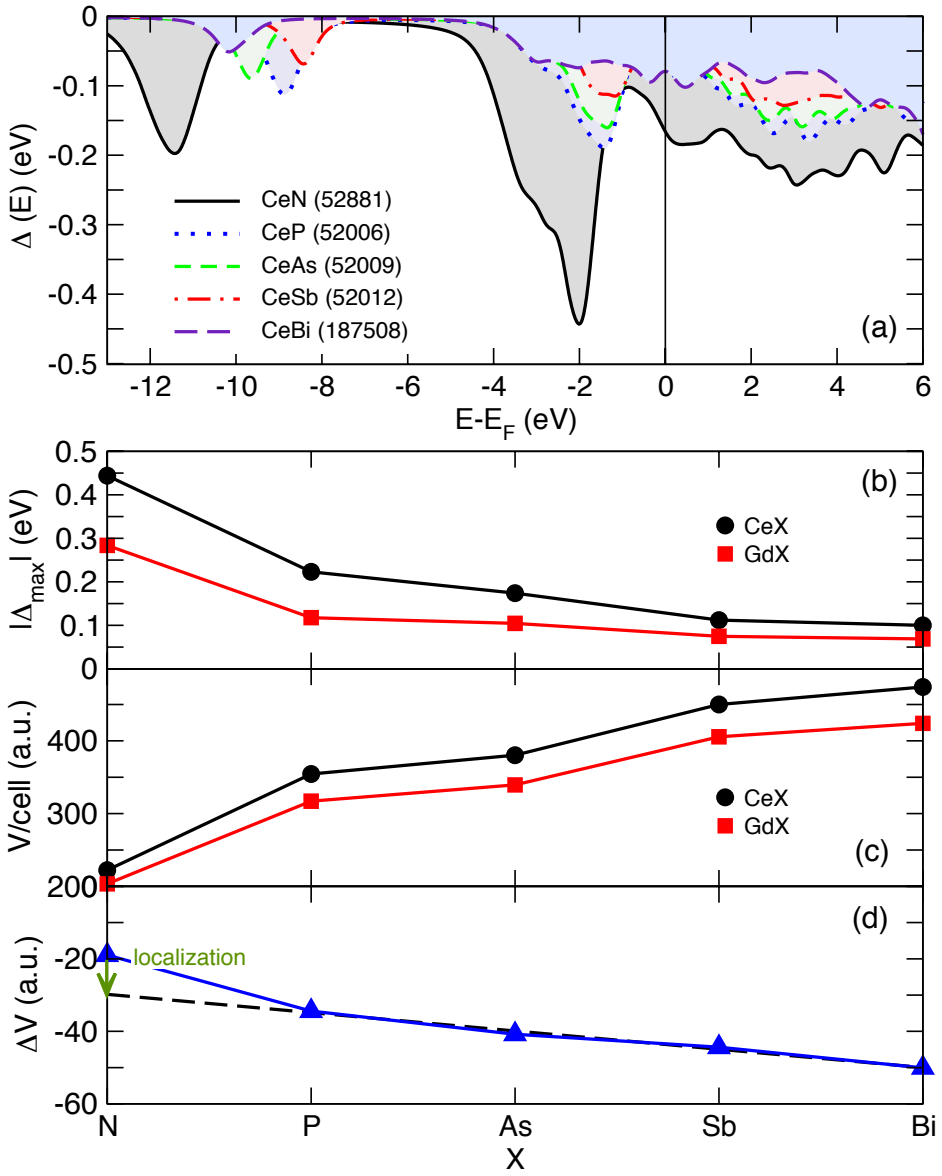

FIG. 1: Calculated hybridization function Δ depending on the energy relative to the Fermi level E_{F} for a series of Ce (a) mono-pnictides. The numbers in the brackets denote the ICSD reference numbers[29]. (b) shows the maxima of Δ for the systems shown in (a) (circles) compared to the values obtained for Gd pnictides (squares). (c) Volume per unit cell of the same systems obtained experimentally and taken from the ICS database[29]. (d) Difference between the experimental volumes of CeX and GdX (X = N, P, As, Sb, Bi) $\Delta V = V(CeX) - V(GdX)$. The dashed black line denotes a linear fit of ΔV(CeX) excluding the N system. The difference between the actual volume V(CeN) and the fit reveals the itinerant character of CeN.

known Ce monopnictides, CeX (X = N, P, As, Sb, Bi), that form in the NaCl structure. It may be observed that CeN shows a distinct peak about 2 eV below the Fermi level and the area under the curve (shaded in gray) up to E_{F} is 4 times larger than for CeBi or CeSb, which both possess a broad but flat $\Delta(E)$ curve. The $\Delta(E)$ of CeP and CeAs lie in-between, reflecting the fact that the 4f states are not as localized as in CeBi nor as delocalized as in CeN. Instead the 4f electron orbitals overlap partially with the valence electrons of the ligand atoms. This trend is in perfect accord with known information about these compounds, e.g. as discussed in Ref.9, and we conclude that for the Ce mono-pnictides, the hybridization function captures well the trends of the degree of localization. Similar trends are observed when Ce is replaced by Gd, although the absolute value of the hybridization is strongly reduced for Gd compounds, with the maximum value ($E < E_{\mathrm{F}}$) being only 65% of the hybridization of the corresponding Ce mono-pnictides. This is consistent with the more localized electron behavious of the Gd compounds (see supplemental material).

Furthermore, for Ce mono-pnictides it has been found that increasing localization of the 4f electron is correlated to the lattice constant,[33] which in itself is natural since larger distance between Ce and neighbouring elements will lead to a reduced interaction. In Fig.1(c) this trend is obvious for the Ce pnictides. As one goes down the group the volume is increasing, whereas the hybridization function drops with a factor of 4-5 1(b). In trying to elicidate this trend in more detail, it becomes relevant to make a comparison to compounds that are known to have completely localized 4f states, namely Gd pnictides. Comparing the experimental volumes of Ce mono-pnictides CeX (X = N, P, As, Sb, Bi) with ones of the corresponding Gd systems confirms the itinerant character of CeN. For both Gd- and Ce-based pnictides the volume shows some irregularities when different ligand atoms among group 15 are considered, with an overall trend of increased volume for the heavier ligands. This trend reflects to some degree the change of the nature of the 4f states, but also the difference in size of group 15 elements. In order to isolate the effect coming from the 4f states we compare the volume of Ce-pnictides with the volume of corresponding Gd-pnictides, in which it is well known that the rare-earth element is trivalent with a fully localized, non-hybriding 4f shell. The difference in volume between these sets of compounds is shown in Fig.1(d). Since the lanthanide contraction is know to result in smaller volumes of heavier rare-earth elements, the difference in volume between CeBi and GdBi may be seen as a refection of this fact. If the nature of the 4f shell of the remaining Ce-pnictides was

completely localized, giving rise to trivalency and chemically inert 4f states, the difference in volume of CeBi and GdBi would be exactly the same for all compounds plotted in Fig.**??**(d). The deviation from this behaviour signals the increased interaction between the 4f states and the ligand orbitals as one moves from heavier to lighter elements of group 15, and it is seen that the deviation behaves almost linearly. The deviation of the ΔV curve from the linear behavior is marked by a dashed line in Fig.**??**(c), and is due to a drastic change in the electronic structure of CeN, compared to the other compounds. In short, this marked deviation is caused by the itinerant character of the 4f electron in CeN.

The data in Fig.1(b)-(d) suggest that the hybridization function is a good measure when trying to identify general trends of the electronic structure of Ce-pnictides. To elucidate whether this observation holds also for other Ce compounds the hybridization function has been calculated for a large set of known Ce compounds, with different symmetry and composition. The hybridization functions of $CeRh_3$ and $CePt_3$ are found to posess distinct peaks at 1.21 eV and 2.53 eV below the Fermi level (Fig. S2). The largest values $|\Delta(E)_{\max}|$ amount to 0.67 eV and 0.57 eV, respectively (cf Table I where we list peak values of several considered compounds). CeN, $CeRh_3$ and $CePt_3$ are known to have itinerant 4f electrons, which is consistent with the large values of $|\Delta(E)_{\max}|$.[34,35] In contrast, $CeCoIn_5$ is an example of a very weakly hybridized compounds, with a $\Delta(E)$ that possess weak, broad features without distinct peaks, (cf pink dash-dotted curve in Fig. S2). This is hinting to a very pronounced localization of the 4f shell, as expected from the literature.[36] Table I suggests that Ce_3Ge and $CeCoIn_5$ are the least hybridized compounds, with expected localized electron behavior. It also shows a large group of intermediate hybridization among these compounds, as exhibited by $CeRu_2Si_2$, CePtIn, $Ce_3Bi_4Pt_3$, $CeNi_2$, $CePt_2$ and $CePt_5$. Experimental data for $CeRu_2Si_2$, a well known heavy fermion material, is consistent with this, check CePtIn and the others.....comment on alpha and gamma ce....comment on Ce2O3....

The discussion above suggests that $\Delta(E)$ can be viewed as a measure for the degree of localization of the Ce 4f electron and can therefore be used to classify various Ce compounds in terms of the degree of localization. However, since we aim to compare $\Delta(E)$ for many systems, the full energy dependent hybridization function may not be a practical gauge. As an alternative we explore the maximum value of $\Delta(E)$ for $E \leq E_{\rm F}$, see Tab. I and Fig. **??**(a) for Ce and Gd mono-pnictides. Another slightly more accurate choice is to integrate over Δ using $|\Delta_{\rm int}|(E_{\rm F}) = \int_{\infty}^{E_{\rm F}} \Delta(E)dE$, cf Tab. I. We will see later that the choice of how

to compare the hybridization function has some influence on the grouping of the systems depending on the degree of localization, but overall trends are picked up by any of the here explored choices. However, from Tab. I we note that $|\Delta_{\rm int}|(E_{\rm F})$ seems to give a better representation of the level of itineracy. For instance, this measure puts $CeNi_2$ on a more itinerant side, which is consistent with the analysis of e.g. Ref.20.

TABLE I: Maxima of the 4f hybridization function of selected reference systems

System	Crystal structure	Space group	$\lvert\Delta_{\rm max}\rvert(E \leq E_{\rm F})$	$\lvert\Delta_{\rm int}\rvert(E_{\rm F})$
Ce (α)	cubic	F m -3 m	0.278	0.518
Ce_3Ga	cubic	P m -3 m	0.073	0.090
Ce_3Ga	cubic	P m -3 m	0.073	0.090
$CeCu_2Si_2$	tetragonal	I 4/m m m	0.111	0.555
$CeCoIn_5$	tetragonal	P 4/m m m	0.113	0.338
$CeRu_2Si_2$	tetragonal	I 4/m m m	0.135	0.608
$Ce_3Bi_4Pt_3$	cubic	I -4 3 d	0.162	0.543
$CePt_5$	hexagonal	P 6/m m m	0.172	0.696
$CePt_2$	cubic	F d -3 m S	0.186	0.771
CePtIn	hexagonal	P -6 2 m	0.235	0.559
$CeNi_2$	cubic	F d -3 m S	0.283	0.903
Ce_2O_3	trigonal	P-3m1	0.629	1.428
$CePt_3$	cubic	P m -3 m	0.569	1.554
$CeRh_3$	cubic	P m -3 m	0.674	1.799

B. Hybridization in cubic binary Ce compounds

We have shown above, for a representative subset of systems, that the hybrizidation function is a reliable criterion to distinguish localized and de-localized systems, even for a rather simple level of approximation as regards the calculation of the electronic structure. Using plain DFT (GGA) calculations, $\Delta(E)$ has been calculated for all known (366, according to

ICSD[29]) binary cubic compounds. Instead of plotting $\Delta(E)$ over the whole energy range, the extrema of the hybridization function below E_{F} are given in Fig.2. Even though there is a certain spread in the data points due to differences in lattice parameters, caused by differences in the experimental techniques and conditions extracting them (such as temperature and external pressure), the trend observed for the systems discussed in the previous sections, seems to cary over to all investigated cubic binary Ce compounds. Fig. 2 shows that the hybridization function has a spread over a large interval, and that compounds that are well established as either localized or itinerant, naturally find their place in the figure in regions with low and high hybridization, respecively. The transition region is drawn in the figure to not be sharp and covers elements that nornally are associated with pronounced Kondo or mixed valence behaviour.

Olles comment: I think we should include in this plot all numbers we have, including e.g. ceP. I also think we should use $|\Delta_{\mathrm{int}}|(E_{\mathrm{F}})$ it seems better to me. We should add data for gamma and alpha Ce as well, as well as Kondo couplings for the systems we have.

We now make a connection to traditional measures of the level of itineracy; the 4f bandwidth and its relation to the Coulomb U. Cubic CeO_2 has, in LDA theory, a very broad 4f band which stretches over 3 eV which strongly hybridizes with the O p orbitals (cf Fig. S3(a)). For CeN, the pnictide with the most itinerant character, the picture is very similar, except that there is no band gap (see Fig. S3(b)). However, even though the width of the 4f band is very similar to that of CeO_2, the overlap between Ce f and N p is smaller compared to the oxide. Going down the N main group (V) the width of the 4f band, as obtained from LDA theory, decreases (as can be seen from Figs. S3(c) and (d)) and the tendency for electron localization becomes stronger. In fact, only the 4f DOS of CeN and CeO_2 have widths that are comparable or larger than the Hubbard U (or even Hubbard U divided by the square root of the degeneracy of the 4f level), which according to conventional criteria would render only these two compounds as being itinerant. The values of $|\Delta(E)|$ gives entirely consistent conclusions regarding how to divide itinerant 4f compounds from the ones with 4f localization. We conclude that the hybridization function is a new and simple measure for how to quantify the level of localization of the 4f electrons in Ce compounds, and that it is advantageous over the DOS function for high throughput screening investigations. It gives in addition important parameters for many-electron physics, and establishes a coupling between ab-initio electronic structure theory and many-body model Hamiltonians, in

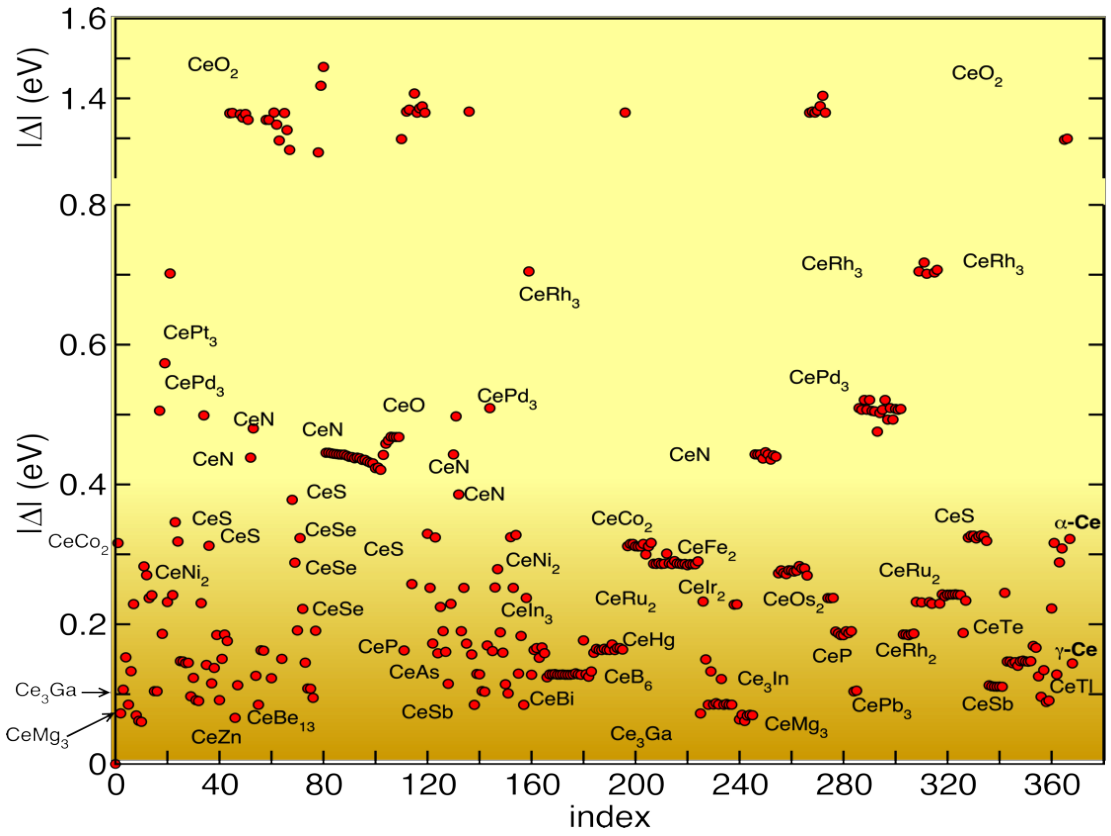

FIG. 2: Maximum values of the hybridization function Δ for 366 binary cubic Ce compounds. The color scale indicates the degree of localization versus itineracy, where blue color represents increased level of localization and red color represents increased itineracy. The index on the x-axis just numbers the systems and has no physical meaning.

this case the single impurity Anderson Hamiltonian.

C. Correlation between hybridization and lattice parameter

The goal of the present paper is not only to classify Ce compounds regarding their itinerant character but to link this information to another tuneable quantity. If this link can be established with a sufficient accuracy it will open a route to design systems with desired electronic properties.

The discussion of the mono-pnictides in Sec. III A has shown that the lattice parameter increases in the same steplike manner as the localization decreases, see Fig. 3(a) and (b). Therefore, the lattice parameter seems to be a suitable quantity to link with the hybridization

function. This is supported by the fact that $|\Delta(E)|$ changes in the same way if the lattice constant of one compound changes due to temperature or pressure as can be seen in Fig. 3(a) and (b) (circled areas) for CeN or $CeRu_2$ for which different data sets with different lattice constants exist.

The volume per atom V/N or more precisely the radius of V/N $r_N = (4\pi r_N^3)/3$ for all investigated compounds is given in Fig. 3 (a). for comparison the corresponding hybridization extrema is also plotted(b). Since the compositon of the systems and the alloy partners are very diverse the radii stretch over a broad region from 2.5 to 4.0 a.u. However, one can already spot some trends as for example the very small volumes of the CeO_2 systems ($r_N \approx 2.75$ a.u.) or the large r_N of $CeMg_3$ which has one of the smallest $|\Delta(E)_{\max}|$ values, cf Fig 3. Visual inspection of Fig. 4 where $|\Delta(E)_{max}|$ is directly plotted versus r_N reveals at least qualitatively a correlation between the two quantities. The hybridization function decays basically with $1/(a + b * r_N)$ whereby a and b are fitting constants. Taking into account all data points except the ones for CeB_6 and $CeBe_{13}$ into account the solid black line in Fig. 4 represents the correlation between the hybrizidation function and the volume. The two systems – CeB_6 and $CeBe_{13}$ – have been excluded from the fit because the for them r_N is an ill-defined quantity. Due to the fact that the ratio between Ce and B or Be is 1:6 and 1:13, respectively the lattice parameters are determined by the light atom and is no contradiction to the overall trend. For CeH_2 with the even smaller hydrogen atom r_N is about 2.858 a.u. and $|\Delta(E)_{\max}|$ corresponds to 0.223 eV which matches the overall trend since H is not the dominating constituent in this material.

A more detailed inspection of Fig. 4 reveals that the overall behavior for all systems is the same but the slope can be different for different classes of systems. CeO_2 seems to form one group including also some CeZ (Z = S, Se, Te) (cf. red dashed-dotted line (I) in Fig. 4). Another group (III) is formed by the mono-pnictides (green dashed line in Fig. 4). Systems of the type CeM_2 (M = 3d transition metal) decay with a different slope (III) and can be viewed as a third group together with Ce compounds with light metals such as Al. The CeT_3 (T = Pt, Pd, Rh) systems do not fit in any of these groups indicated by the blue line in in Fig. 4. This suggests that besides the obvious decay of $|\Delta(E)_{\max}|$ with r_N there might be a more subtle dependence which determines the slope (IV). This brings up the question what causes these different slopes or the fine-structure in the $1/r_N$ decay? The above defined groups differ in the electronic structure i.e. the type of valence electrons and their parity

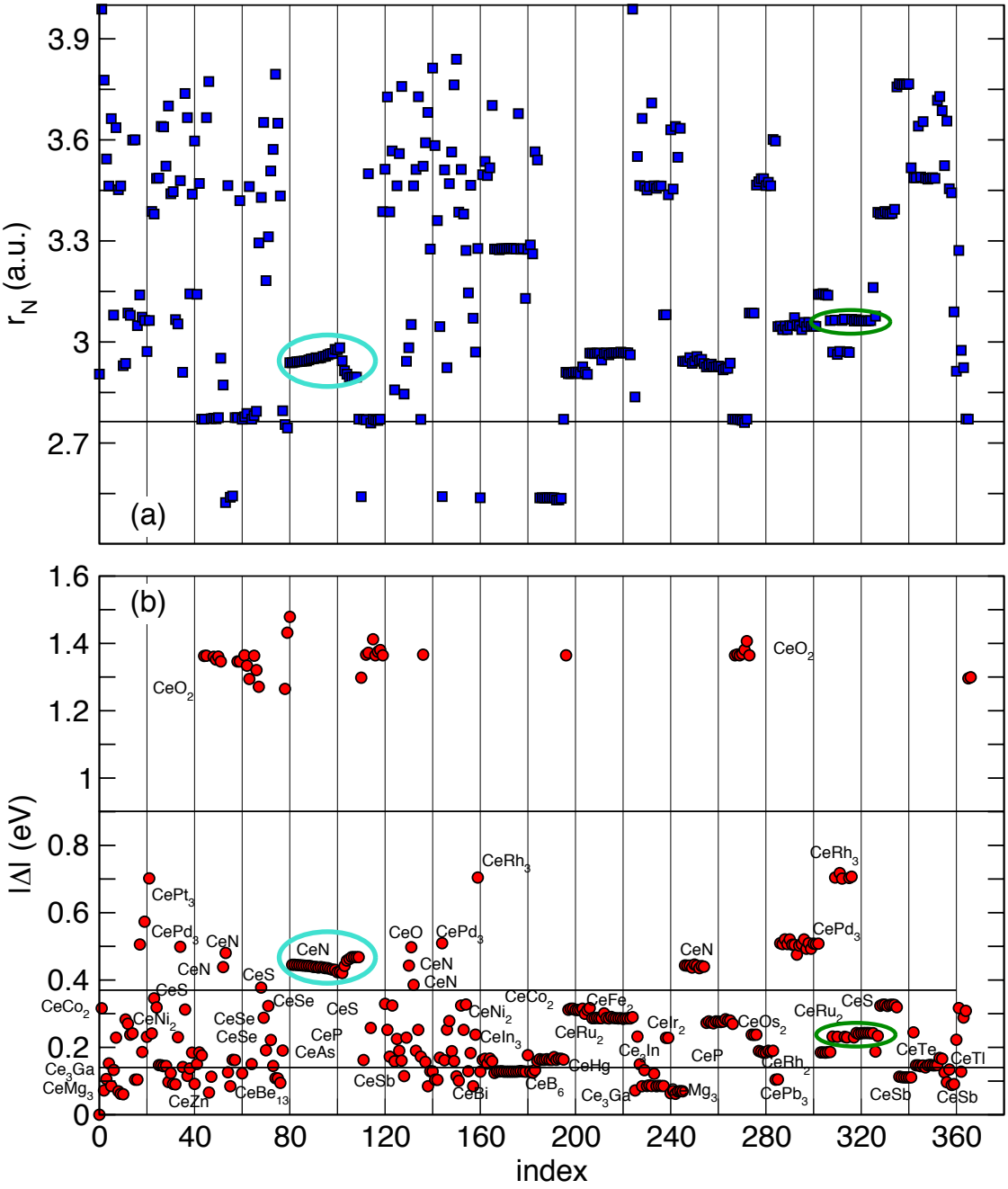

FIG. 3: The radius of the experimental volume per atom r_N for cubic binary Ce compounds (a) and the maxima of the hybridization function $|\Delta(E)|(E \leq E_{\mathrm{F}}$ for the same set of compounds (b). The circles areas mark sets of CeN and $CeRu_2$ systems indicating an inverse relation between the volume and the size of the hybridization. For more details see text.

and the width of the valence bands seem to be important factors. CeO_2 as well as CeZ (Z = S, Se, Te) have nominally p^4 valence electrons from the non-Ce element and which have the

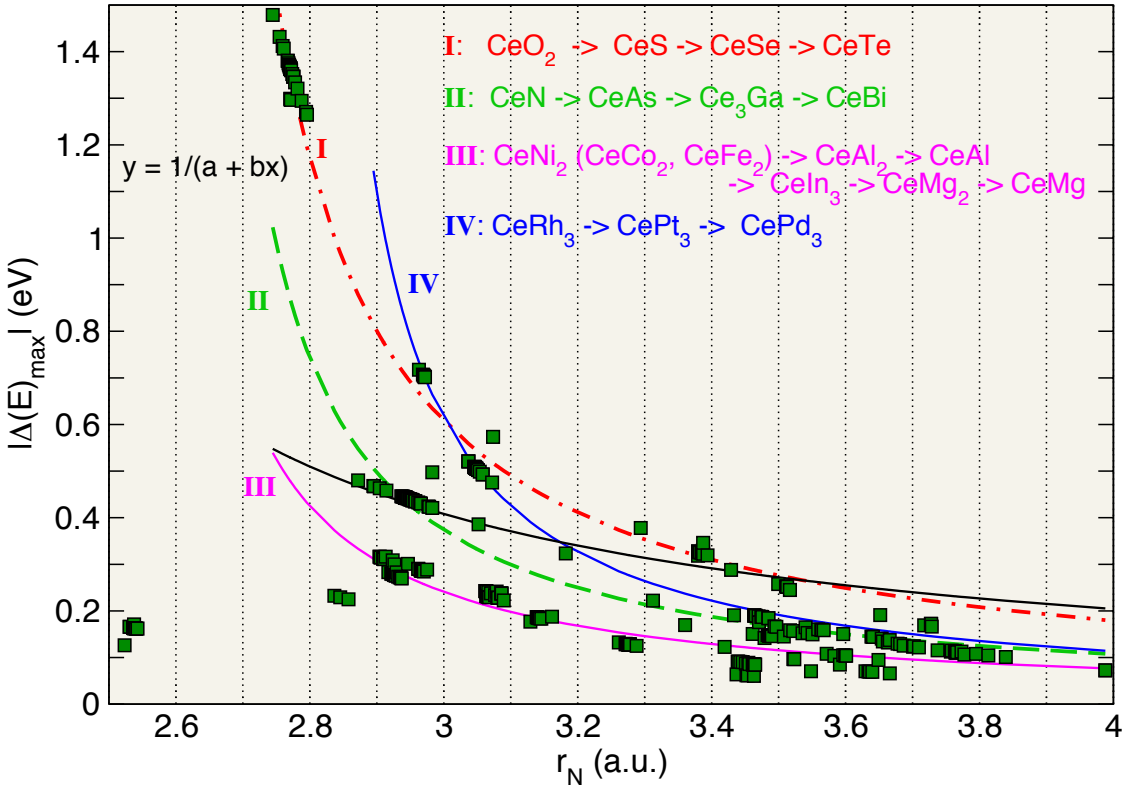

FIG. 4: Scatter plot of the absolute values of the hybridization function $|\Delta E_{max}|$ versus the radius of the volume per atom. r_N The lines are inverse linear fits. The solid black line represents the fit over all data sets except the ones for CeB_6 aqnd $CeBe_{13}$ for details see text.

same parity as the Ce f electron. Therefore, these electrons are likely to hybridize which is reflected in the large values of the hybridization function. Even though the r_N of the CeZ is already quite large the $|\Delta(E)_{\rm max}|$ lies clearly above all other systems with similar volume, see Fig. 4. With decreasing number of p electrons the slope increases and the overall size of the hybridization becomes smaller as can be seen for the p^3 systems which contain the mono-pnictides (green dashed line). Systems without a significant p contribution to the valence electrons form the lowest group (pink curve in Fig. 4). These class has basically s or 3d valence electrons which have opposite parity then the f electrons and consequently the tendency to hybridize with the f type electrons is much lower. The fourth group is special since the T elements (T = Pt, Pd, Rh) also possess mainly d type valence electrons but at the same time they have comparable large hybridization energies. One difference between the CeT_3 and the CeM_2 compounds is that due to 3(4)d core electrons the outer d electrons are nearly free and form slightly broader bands[37] which then leads to a larger

hybridization with the f electron. Besides the different core structure these compounds have three 4d or 5d atoms per formula which multiplies the effect. CeT_2 (T = Pt, Pd, Rh) do not show the same behavior. Their $|\Delta(E)_{\max}|$ values are much smaller and they fit in the 3d group. Now one might think that CeT_x compounds with larger x values would lead to even higher hybridization energies. But for example the r_N of $CePt_5$ amounts to 3.08 Å but its hybridization is with 0.172 eV small compared to the one obtained for $CePt_3$ (see Tab. I). However, $CePt_5$ crystallizes in a hexagonal structure (space group no. 191) and the different geometrical arrangement has certainly an influence on the hybridization of the orbitals.

Summarizing, we observe a clear correlation between the size of the hybridization function and the inverse of volume or the radius of the volume. In addition, we discovered a fine structure within the Ce compounds, i.e. the slope of the decay is also determined by the electronic configuration of the non-Ce element. Together these two findings might be used for the search of new Ce systems, whereby the overall dependence of the hybridization function on the volume gives a first indication how to tune the volume to obtain a more itinerant or localized electron system. For a fine tuning the type of valence electrons might be chosen accordingly.

To confirm the presumably existing correlation quantitatively a statistical analysis of the $r_N(i)$ and $\Delta(E)_{\max}(i)$ (for simplicity we skip E in the following) data sets has been performed, where i is the sample index. We use Pearson's correlation coefficient $\rho(r_N, \Delta)$ [38,39] and mutual information theory $I(r_N, \Delta)$ in order to quantitatively estimate the correlated or anti-correlated nature of the two data sets. In Fig. 4(a) and (b), we present the distribution of 366 Ce based compounds in the volume and hybridization energy range correspondingly. The histogram distribution is created using 25 bins for both given ranges of volume/atom (2.5 Å^3 to 4 Å^3) and hybridization energy (0.0 to -1.5 eV). The probability of the i-th bin for a r_N data set is obtained using

$$P_{r_N}(i) = \frac{n_{r_N}(i)}{L}, \tag{2}$$

where $n_{r_N}(i)$ is the number of compounds in the i-th bin, and L is the total number of compounds in the volume data set. Similarly, the probability of the j-th bin in the hybridization data set is given by

$$P_{\Delta}(j) = \frac{n_{\Delta}(j)}{L}. \tag{3}$$

The correlation coefficient which corresponds to the scatter plot of $r_n(i)$ versus $\Delta(i)$

shown in Fig. 5 can be determined by using

$$\rho(r_N, \Delta) = \frac{\sum_{i=1}^{L}(r_N(i) - \bar{r}_N)(\Delta(i) - \bar{\Delta})}{\sqrt{(\sum_{i=1}^{L}(r_N(i) - \bar{r}_N)^2)(\sum_{i=1}^{L}(\Delta(i) - \bar{\Delta})^2)}}. \quad (4)$$

Here $\bar{r}_N$ and $\bar{\Delta}$ are the average volume/atom and average hybridization for the L Ce-compound data set. Though we have performed calculations for 367 data sets the actual number of different compounds is 52 because many systems have been investigated under different conditions. Thinking of predicting materials properties the smaller data set is more suitable since it contains only composition dependent information. We also performed the analysis for the large set which includes information on the volume dependence of single compounds. The latter value will be given in brackets. We find a correlation coefficient of $\rho(r_N, \Delta)$ = -0.5437 (-0.5615). Since ρ varies by definition between 1 (total correlation), 0 (no correlation), and -1 (maximal anti-correlation) this clearly indicates that the correlation between our two properties r_N and Δ is at the boarder line of the moderate and strong anti-correlation regime.

In Fig. 5, we plot the two-dimensional heat-map of $r_N(i)$ and $\Delta(i)$ data sets. The color scheme indicates the population of Ce compounds in each cell. The heat-map provides information on the joint probability distribution $P(i, j) = n(i, j)/L^2$, where $n(i, j)$ is the number count in the i, j-th cell, and L=52 is the total size of the data set. This quantity is essential to determine the *mutual information*. Unlike the correlation coefficient, the mutual information is a positive definite quantity which provides a measure of the *information entropy*, and therefore, quantifies the amount of information that can be achieved for one random variable through another set of random variables. Formally, the mutual information is defines as

$$I(r_N, \Delta) = \sum_{i \in r_N, j \in \Delta} P(i, j) \log\left(\frac{P(i, j)}{P(i)P(j)}\right), \quad (5)$$

where i and j indices stand for the i-th row j-th column (i, j-th cell) in the heat-map. For our given data set of r_N and Δ, the mutual information is $I(r_N, \Delta) = 0.4152$ (0.7332). This value of $I(r_N, \Delta)$ clearly demonstrates a quite high predictive nature of electron-electron correlation from only volumetric data and vice versa, and thus opens up pathways for machine aided new materials design principles. The value for the large data set points to an even higher predictive power which basically reflects the fact that the localization within a material is strongly related to the volume.

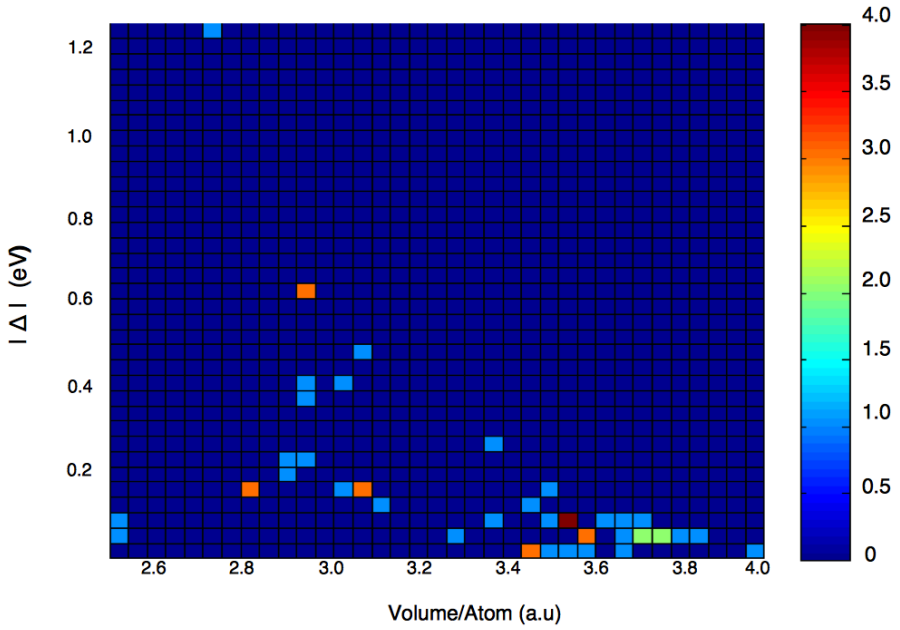

FIG. 5: Twodimensional heat-map obtained from Eq. III C where colors represent the number-count of Ce compounds in each cell. Data are shown for the $L = 52$ data set which contains only unique systems.The color bar quantifies the color schemes used in this plot. The heat-map provides joint probability distribution and measures mutual information $I(v, \Delta)$ (see text for details).

D. Kondo couplings and Kondo temperature

In the previous part of the paper we have convincingly demonstrated that the hybridization function can be used as a measure for the degree of localization in a Ce-compound. The localized 4f electrons give rise to the Kondo effect, i.e. they form scatter centers for the other valence electrons and lead to the experimentally observed minimum of the electrical conductivity. Knowing from Andersson's impurity model that the Kondo coupling and the Kondo temperature depend on the hybridization energy, it is obvious to check whether the calculated hybridization functions Δ can reproduce the Kondo physics of Ce compounds. To describe the Kondo temperature T_{K} and the Kondo coupling parameter J_K different approaches are used. Here we follow the model used in by Lethuillier and Lacroix-Lyon-Caen.[40,41] which is based on the Andersson impurity model. Eq. 2 in Ref. 40 states that the

Kondo temperature of a Ce compound can be written as

$$T_{\mathrm{K}} \;=\; \alpha \,\exp\left[\frac{2}{(2J+1)J_{\mathrm{K}}\,\rho(E_{\mathrm{F}})}\right] \tag{6}$$

here $\rho(E_{\mathrm{F}})$ corresponds to the DOS at the Fermi level with the 4f electron being treated as core electron, $J = 5/2$ for tripositive Ce ions and the probability factor α. The Kondo coupling parameter J_{K} is given by

$$J_{\mathrm{K}} \;=\; \frac{2\Delta^2}{(E_f - E_{\mathrm{F}})} \tag{7}$$

with Δ being the hybridization energy (mixing parameter of the Andersson model). The energy difference in the denominator denotes the distance of the 4f peak from the Fermi level. Since the purpose of this paper is to use data mining to find relations out of a big amount of data we do not aim to predict the precise T_{K} for a single system but find general trends. Therefore, we use for all investigated systems obtained $(E_f - E_{\mathrm{F}})$ which was obtained for α-Ce namely 3 eV [42] and consider the following relation instead where the constant α is neglected

$$\ln T_{\mathrm{K}} \;\sim\; \frac{1}{2\,\Delta^2(E_{\mathrm{F}})\,\rho(E_{\mathrm{F}})} \tag{8}$$

with $J = 5/2 and \Delta(E_{\mathrm{F}})$ being the value of the hybridization function at the Fermi level, which is in most cases considered here identical to the maximum. In contrast to the previous discussion of the relation between Δ and the volume (see Sec.III B) now also the density of states has to be taken into account. Both data (Δ and ρ) are provided by the IMS database. Plotting the calculated data versus the experimental Kondo temperatures corresponding to the relation in Eq. 8 we expect a linear behavior. However, most Kondo temperatures are given as a range, e.g. for CeBi 10-20 K[43] or regarding to Ref. 44 all Ce monopnictides should have Kondo temperatures between 50 and 100 K. This cannot simply be interpreted as an error bar because the values arise from different experimental methods and model assumptions. Therefore, in Fig. 6 we provide two data sets one containing the smallest T_K (small red circles in Fig. 6) found in literature and one for the largest as well (large blue circles in Fig.6).

Fig. 6 reveals indeed the expected linear behavior between the logarithm of the experimental Kondo temperatures and the calculated values $(\rho(E_F)\Delta^2(E_F))^{-1}$. The spreading of the data is partially related to the experimental Kondo temperature which are obtained from different measurement techniques, e.g. from magnetic susceptibility measurements [40,51] or

TABLE II: Experimental Kondo temperatures $T_{\rm K}$, the calculated hybridization energies $\Delta(E_{\rm F})$ (eV), the corresponding calculated total DOS at the Fermi level (with the 4f electron being treated as core electron) $\rho(E_{\rm F})$ (states/eV) are given for several cubic binary Ce compounds. The distance between the Fermi level $E_{\rm F}$ and the position of the 4f peak E_f (eV) is assumed to be 3 eV.

System	ICSD	$\|\Delta(\mathrm{E_F})\|$	$\rho(E_F)$	$(\rho\Delta^2)^{-1}$	$T_{\rm K}$ (max)	$T_{\rm K}$ (min)
α-Ce	(41823)	0.322	0.617	15.64	2000[45]	1000[46]
$CeAl_2$	(606387)	0.129	1.417	42.41	15[47]	0.19[41]
CeB_6	(612731)	0.124	0.408	159.39	7.7[48]	3[48]
CeBi	(187508)	0.079	1.160	138.13	100[44]	10[43]
$CeFe_2$	(620998)	0.226	4.963	3.94	500[49]	500[49]
Ce_3In	(621360)	0.124	2.561	25.40	17[50]	17[50]
$CeIn_3$	(621361)	0.086	0.957	141.24	1.7[41]	1.7[41]
$CeMg_3$	(621498)	0.062	1.271	204.68	4[51]	3[51]
$CeNi_2$	(102229)	0.174	0.779	42.40	>1000[52]	>1000[52]
$CePb_3$	(621777)	0.104	1.343	68.84	0.002[40]	0.002[40]
$CePd_3$	(107546)	0.054	0.262	1308.91	350[52,53]	240[52,53]
$CeRh_2$	(621938)	0.150	0.579	76.76	400[54]	>300[53]
$CeRh_3$	(604325)	0.174	2.152	15.35	1350[52]	1350[52]
CeSb	(52012)	0.112	0.121	658.84	100[44]	30[43]
Ce_3Sn	(622247)	0.146	2.488	18.86	40[50]	40[50]
$CeSn_3$	(622224)	0.146	1.231	37.57	200[53]	100[53]

trends can be obtained from resistivity curves [55]) as well as the quality of the samples (single crystals [56], polycristalline samples [57], nanocrystals [58]) used plus the fact that the calculated values are on a simple GGA footing. However, the overall trend is clearly reproduced. Heavy fermion systems such as CeB_6 and $CeMg_3$ provide large $(\rho(E_F)\Delta^2(E_F))^{-1}$ which are connected to small T_K, with decreasing $(\rho(E_F)\Delta^2(E_F))^{-1}$ $\ln T_{\rm K}$ increases, i.e. the heavy fermion character vanishes and finally the smallest $(\rho(E_F)\Delta^2(E_F))^{-1}$ values are obtained

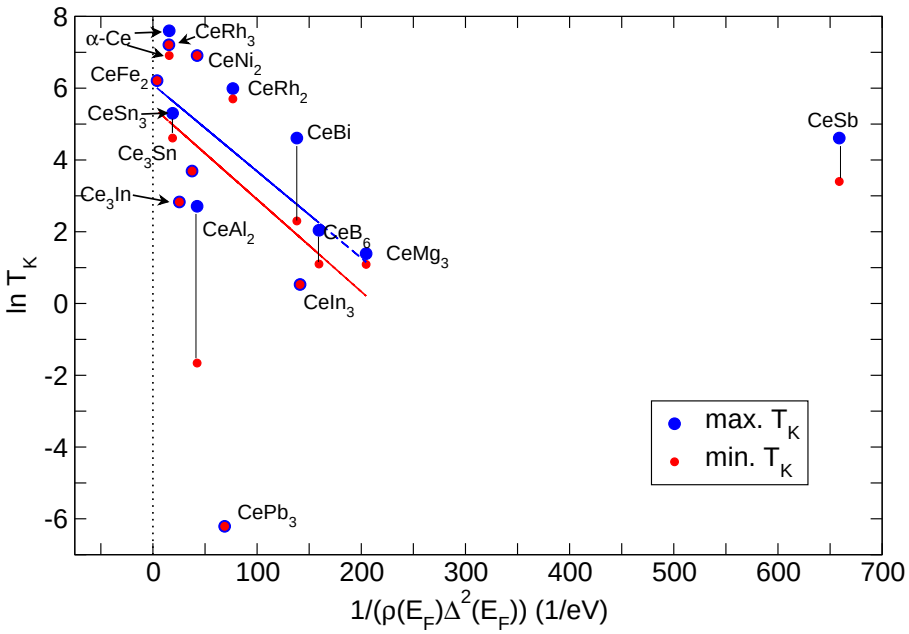

FIG. 6: Relation between the calculated hybridization function $\Delta(E_{\mathrm{F}})$ and Kondo temperatures obtained from lierature for known cubic binary Ce compounds. The hybridization function $\Delta(E_{\mathrm{F}})$ is weighted by the spd-DOS $\rho(E_{\mathrm{F}})$. Both values are taken at the Fermi level E_{F}. The vertical black lines are guides to the eye connecting the T_{K} min and T_{K} max of a system.

for Pauli-like compounds such as $CeRh_2$ and $CeNi_2$. Systems which seem not to follow the trend are CeSb and $CePb_3$ (not shown in the figure) cf Fig. 6 and Tab II. Both systems are barely metallic and provide a very small DOS at the Fermi level together with the small hybridization at the Fermi niveau $(\rho(E_F)\Delta^2(E_F))^{-1}$ basically diverges. In case of CeSb the vanishing DOS(E_{F}) agrees with findings from literature and has been obtained from a DFT+U study, see Ref. 59. $CePd_3$ has a pseudo gap at the Fermi level with intrinsic gap states and can be viewed as a Kondo insulator.[60] The other extreme case which seems not to fit in the picture is $CePb_3$ for which a Kondo temperature of 0.002 K has been obtained from magnetic susceptibility measurements fitted to the Lethuillier model. [40] This point has also not considered in the linear fits. Summarizing, the calculated hybridization functions in connection with the corresponding DOS are also in line with the Kondo physics reflecting the expected exponential behavior and according to that Fig. 6 can serve as an approximate

guideline whether a material can really be viewed as a Kondo system since systems with vanishing T_K or energy gaps are far away from the linear fit and can be ruled out easily.

IV. SUMMARY AND CONCLUSION

Aiming to identify routes to predict materials properties such as the itinerant or localized character of 4f compounds we did data mining within exisitng (mostly cubic binary) Ce compounds analyzing the hybridization of the Ce 4f electron with the valence electrons of the system. Since the strength of the hybridization between the 4f and the valence electrons of the non Ce constituent defines in large parts whether the material will be an itinerant or localized electron system, the hybridization function can be viewed as a tool to classify the compounds. The localized/itinerant character of known the is clearly reflected in the calculated hybridization energies, not only for cubic systems but also for materials with different lattice structure which have been included as test systems. With regard to the search for new materials the hybridization function could be a suitable measure hence it is much easier to handle and to utilize than the density of states. Thinking of the developing field of computational materials design such an easy classification method is very welcome. However, to make use of it we had to link the hybridization to a second quantity which can be tailored by composition or strain if grown on a surface. Here, the volume was a natural choice because of the well-known volume dependence of the Ce mono-pnictides. Indeed our results show a strong anti-correlation between the hybridization and the volume or the radius of the volume and a medium to high predictive power. Interestingly enough the besides the general inverse relation between volume and hybridization the results show a fine-structure depending on the parity of the non Ce valence electrons. The absolute values of the hybridization tend to be higher for systems with mostly p valence electrons such as CeO_2 or CeSe whereas for systems with s and d valence electrons like $CeTM_2$ (TM = 3d transition metal) the hybridization is lower.

Since the hybridization energy is an essential part of the Kondo coupling constant it was assumed the trends of the Kondo behavior should be reflected in the calculated data. Indeed we were able to show that the calculated hybridization combined to the DOS agrees with the experimental findings for the Kondo temperature following the relation $\ln T_K \sim 1/(\Delta^2(E_F)\,\rho(E_F))$. From the systems investigated so far it seems obvious the outliers, i.e.

systems which do not show the linear dependence are not really metallic Kondo compounds.

The three observations – the anti-correlation, the valence electron dependent fine-structure as well as the trends found for the Kondo temperature might be used to find materials with desired properties. However, the purpose methods is to reveal trends, the absolute numbers should be handled with care since they depend on the DFT level used in the study. In order to improve the quantitative accuracy further calculations beyond the GGA have to be done.

Acknowledgements

O.E. and H.C.H. would like to thank Anna Delin for helpful discussions on the Kondo physics of the systems. We acknowledge financial support from the Swedish Research Council. O.E Acknowledged support from KAW (projects 2013.0020 and 2012.0031). H.C.H. acknowledges financial support via STandUP. The calculations were performed at NSC (Linköping University, Sweden), PDC (KTH, Stockholm, Sweden), HPC2N (Umeå University, Sweden) under a SNAC project and at LANL facilities.

---

[1] J. Kašpar, P. Fornasiero, and M. Graziani, Catalysis Today **50**, 285 (1999).

[2] C. W. Brooks, *Understanding lens surfaces* (Butterworth-Heinemann, Boston, 1992).

[3] D. W. Coutts and A. J. S. McGonigle, IEEE Quantum Elec. **40**, 1430 (2004).

[4] N. V. Keis and A. I. Komissarov, Met Sci Heat Treat **5**, 439 (1963).

[5] G. A. R. N. S. Kreshchanovskii, V. R. Nazarenko, Met Sci Heat Treat **5**, 444 (1963).

[6] T. G. Harvey, Corrosion Engineering, Science and Technology **48**, 248 (2013).

[7] K. Reinhardt and H. Winkler, *Cerium Mischmetal, Cerium Alloys, and Cerium Compounds* (Wiley-VCH, Weinheim, 2012).

[8] H. H. Hill, in *Plutonium 1970 and other actinides*, edited by W. N. Miner (Met. Sot. AIME, New York, 1970).

[9] J. G. Sereni and O. Trovarelli, J. Magn. Magn. Mater. **140-144**, 885 (1995).

[10] L. de Long, J.G.Huber, and K.S.Bedell, J. Magn. Magn. Mat. **99**, 171 (1991).

[11] W. Metzner and D. Vollhardt, Phys. Rev. Lett. **62**, 324 (1989).

[12] A. Georges and G. Kotliar, Phys. Rev. B B **45**, 6479 (1992).

[13] T. Fujita, T. Suzuki, S. Nishigori, T. Takabatake, H. Fujii, and J. Sakurai, J. Magn. Magn. Mater. **108**, 35 (1992).

[14] J.M.Wills and B.R.Cooper, Phys. Rev. B **36**, 3809 (1987).

[15] B. Johansson, Phil. Mag. **30**, 469 (1974).

[16] A. Delin, P. Oppeneer, M. Brooks, J. Wills, B. Johansson, and O. Eriksson, Phys. Rev. B **55**, 10173 (1997).

[17] B. Johansson and N. Mårtensson, Phys. Rev. B **21**, 4427 (1980).

[18] A. Delin, L. Fast, B. Johansson, O. Eriksson, and J. Wills, Phys. Rev. Lett. **79**, 4637 (1997).

[19] S. Malik and D. Adroja, Phys. Rev. B **43**, 6295 (1991).

[20] A. Böhm, R. Caspary, U. Habel, L. Pawlak, A. Zuber, F. Steglich, and A. Loidl, J. Magn. Magn. Mater. **76& 77**, 150 (1988).

[21] K. Satoh, T. Fujita, Y. Maeno, Y. Uwatoko, and H. Fujii, J.Phys. Soc. Jpn. **59**, 6922 (1990).

[22] M. F. Hundley, P. C. Canfield, J. D. Thompson, Z. Fisk, and J. M. Lawrence, Phys. Rev. B **42**, 6842 (1990).

[23] F. Steglich, J. Aarts, C. D. B. W. Lieke, D. Meschede, W. Franz, and H. Schäfer, Phys. Rev. Lett. **43**, 1892 (1979).

[24] E. Weschke, C. Laubschat, R. Ecker, A. Hohr, M. Domke, G. Kaindl, L. Severin, and B. Johansson, Phys. Rev. Lett. **69**, 1792 (1992).

[25] O. Eriksson, L. Nordström, M. S. S. Brooks, and B. Johansson, Phys. Rev. Lett. **60**, 2523 (1988).

[26] K. L. *et al.*, Science **351**, 1415 (2016).

[27] C.Ortiz, O. Eriksson, and M.Klintenberg, Comp. Mater. Sci. **44**, 1042 (2009).

[28] J. M. Wills, M. Alouani, P. Andersson, A. Delin, O. Eriksson, and O. Grechnyev, *Full-Potential Electronic Structure Method*, Vol. 167 of *Springer series in solid state science* (Springer, Berlin, Germany, 2010).

[29] G. Bergerhoff and I. D. Brown, in *Crystallographic Databases*, edited by F. H. Allen (International Union of Crystallography, Chester, 1987).

[30] T. Björkman, Computer Physics Communications **182**, 1183 (2011).

[31] R. Armiento and A. E. Mattsson, Phys. Rev. B **72**, 085108 (2005).

[32] A. E. Mattsson, R. Armiento, J. Paier, G. Kresse, J. M. Wills, and T. R. Mattsson, J. Chem.

Phys. **128**, 084714 (2008).

[33] M. S. Litsarev, I. D. Marco, P. Thunström, and O. Eriksson, Phys. Rev. B **86**, 115116 (2012).

[34] E. Weschke, C. Laubschat, R. Ecker, A. Höhr, M. Domke, G. Kaindl, L. Severin, and B. Johansson, Phys. Rev. Lett. **69**, 1792 (1992).

[35] L. Severin and B. Johansson, Phys. Rev. B **50**, 17886 (1994).

[36] N. J. Curro, B. Simovic, P. Hammel, P. G. Pagliuso, J. L. Sarrao, and J. D. Thompson, PRB **64**, 180514(R) (2001).

[37] M. Sigalas, D. A. Papaconstantopoulos, and N. C. Bacalis, Phys. Rev. B **45**, 5777 (1992).

[38] K. Pearson, Proc. Royal Soc. London **58**, 240 (1895).

[39] S. M. Stigler, Stat. Sci. **4**, 73 (1989).

[40] P. Lethuillier and C. Lacroix-Lyon-Caen, J. de Physique **39**, 1105 (1978).

[41] C. Lacroix-Lyon-Caen and P. Lethuillier, Phys. Rev. B **15**, 3522 (1977).

[42] A. Delin, L. Fast, B. Johansson, J. M. Wills, and O. Eriksson, Phys. Rev. Lett. **79**, 4637 (1997).

[43] M. SERA, T. SUZUKI, and T. KASUYA, J. Magn. Magn. Mater. **31-34**, 385 (1983).

[44] T. Kasuya, O. Sakai, J. Tanaka, H. Kitazawa, and T. Suzuki, J. Magn. Magn. Mater. **63-64**, 9 (1987).

[45] L. Liu, J. Allen, O. Gunnarsson, N. Christensen, and O. Andersen, Phys. Rev. B **45**, 8934 (1992).

[46] M. B. Zölfl, I. A. Nekrasov, T. P. nad V. I. Anisimov, and J. Keller, Phy **89**, 276403 (2010).

[47] E. Patthey, J.-M. Imer, W.-D. Schneider, H. Beck, Y. Baer, and B. Delley, Phys. Rev. B **42**, 8864 (1990).

[48] S. Suga and A. Sekiyama, *Photoelectron spectroscopy*, Vol. 176 of *Springer series in optical science* (Springer, Heidelberg, 2014).

[49] E.-J. Cho, R.-J. J. B.-H. Choi, S.-J. Oh, T. Iwasaki, A. Sekiyama, S. Imada, S. Suga, T. Muro, J.-G. Park, and Y. S. Kwon, Phys. Rev. B **67**, 155107 (2003).

[50] C. H. Wang *et al.*, Phys. Rev. B **81**, 235132 (2010).

[51] P. K. Das, N. Kamar, R. Kulkarni, and A. Thamizhavel, Phys. Rev. B **83**, 134416 (2011).

[52] P. Weibel, M. Grioni, D. Malterre, O. Manzardo, Y. Baer, and G. Olcese, Europhys. Lett. **29**, 629 (1995).

[53] Y. Ōnuki and T. Komatsaubara, J. Magn. Magn. Mater. **63&64**, 281 (1987).

[54] H. Sugawara *et al.*, J. Phys. Soc. Jpn **63**, 1502 (1994).

[55] Y. Hayashi, S. Takai, T. Matsumara, H. Tanida, M. Sera, K. Matsubayashi, Y. Uwatoko, and A. Ochiai, J. Phys. Soc. Jpn. **85**, 034704 (2016).

[56] F. Venturini, J. C. Cezar, C. D. Nadaï, P. C. Canfield, and N. B. Brookes1, J. Phys. Condens. Matter **18**, 9221 (2006).

[57] R. M. Galera, A. P. Murani, and J. Pierre, J. Physique **46**, 303 (1985).

[58] Y. Chen, P. H. Huang, M. N. Ou, C. R. Wang, Y. D. Yao, T. K. Lee, M. Ho, J. M. Lawrence, and C. H. Booth, Phys. Rev. Lett. **98**, 157206 (2007).

[59] D. L. Price, B. R. Cooper, S.-P. Lim, and I. Avgin, Phys. Rev. B **61**, 9867 (2000).

[60] B. Bucher, Z. Schlesinger, D. Mandrus, Z. Fisk, J. Sarrao, J. F. DiTusa, C. Oglesby, G. Aeppli, and E. Bucher, Phys. Rev. B **53**, R2948 (1996).